Advances in Intelligent Systems Research, volume 164
International Conference on Mathematics, Modeling, Simulation and Statistics Application (MMSSA 2018)

A Novel Classification Method for Subsurface Targets

Wupeng Xie, Xiaojuan Zhang* and Yaxin Mu
Key Laboratory of Electromagnetic Radiation and Sensing Technology, Chinese Academy of Sciences
No. 19 North 4th Ring Road West, Haidian District, 100190, Beijing, China
*Corresponding author

Abstract—**In this paper, a novel subsurface targets classification method based on the DE-LM joint inversion technique is presented, which requires few control variables and has strong robustness. It eliminates the inaccuracy of the inversion results when an initial value is far away from the truth value by the Levenberg-Marquardt(LM), and reinforces the weak local search capability of the Differential Evolution(DE) inversion technique. Next, the classification method proposed herein extracts subsurface characteristics of targets and classifies the targets automatically by means of the intrinsic responses of three-dimensional orthogonal magnetic dipole instead of using complex machine learning techniques or setting up the targets library for comparison. The experimental results show that the addition of 15% Gaussian white noise to the synthetic data can still lead to convergence to an optimal solution and classify the subsurface targets quickly and accurately, it demonstrates the effectiveness of the method proposed herein.**

Keywords—time domain electromagnetic method; inversion problems; three-dimensional orthogonal magnetic dipole; subsurface targets classification

I. INTRODUCTION

The time domain electromagnetic (TDEM) method is an artificial source detection approach based on electromagnetic induction, which uses an un-grounding loop source(magnetic source) or grounding line source (electric source) to launch a primary field to the ground, and under its excitation, eddy currents induced in subsurface conductor targets will produce an induced secondary field. The TDEM method satisfies the electromagnetic wave diffusion equation rather than the wave equation as electromagnetic induction (EMI) frequencies range from tens of Hz to hundreds of kHz [1], and it results in the impossibility of forming high-resolution images of the subsurface targets due to the volumetric effect of the diffusion field, and it is impossible to obtain an analytic solution of the secondary field response of arbitrary shape conductors. The amount of computation is too large if we adopt the finite element discrete numerical calculation method and it is not suitable for real-time recognition of the subsurface targets [2].

Since the subsurface detection where the target-sensor distance is 3-5 times the dimension of a target, the EMI responses of the metal targets can be well represented by the induced magnetic dipole fields [3],[4].

In this paper, we use the concentric three-dimensional orthogonal magnetic dipole model to equivalently represent the subsurface metal targets. The equivalent magnetic dipole intrinsic responses of the targets are obtained by using the DE-LM joint inversion technique proposed herein. Subsequently, the characteristic information of the subsurface targets is extracted by using our parameter synthesis method. In Section II, physical modeling is presented. DE-LM joint inversion technique and subsurface targets classification method are discussed in detail. In Section III, the method proposed herein is evaluated using synthetic data, our results demonstrate the method is effective. In Section IV, the method proposed herein is summarized.

II. INVERSION TECHNIQUE AND CLASSIFICATION METHOD

A. Physical Modeling

As a receiving loop, we do not consider the polarity of the induced voltage as a transmitting coil emits a positive and negative alternating primary field. According to the law of Faraday's electromagnetic induction and curl theorem, the induced voltage is expressed as

$$V(\boldsymbol{r}_R, t) = \int_l \frac{\partial A(r_R,t)}{\partial t} \cdot d\boldsymbol{l} \quad (1)$$

where l is the closed boundary of the receiving loop.

The magnetic vector potential $\boldsymbol{A}(\boldsymbol{r}_R, t)$ generated at observation point $\boldsymbol{R}$ by a metal target which is equivalent to a concentric orthogonal three-dimensional magnetic dipole at $\boldsymbol{r}$ is given by

$$\boldsymbol{A}(\boldsymbol{r}_R, \mathrm{t}) = \frac{\mu_0}{4\pi} \cdot \frac{\boldsymbol{m}(t)\times \boldsymbol{r}_R}{|\boldsymbol{r}_R|^3} \quad (2)$$

substituting (2) into (1), we have another form of secondary field response, namely

$$\boldsymbol{V}(\boldsymbol{r}_R, \boldsymbol{t}) = \frac{\boldsymbol{\mu_0}}{\boldsymbol{4\pi}} \int_l \frac{\partial \boldsymbol{m}(t)}{\partial t} \cdot \frac{\boldsymbol{dl} \times -\boldsymbol{r}_R}{|\boldsymbol{r}_R|^3} \quad (3)$$

where $\boldsymbol{r}_R = \boldsymbol{R} - \boldsymbol{r}$, the induced dipole moment $\boldsymbol{m}(t)$ is denoted as [5]

Copyright © 2019, the Authors. Published by Atlantis Press.
This is an open access article under the CC BY-NC license (http://creativecommons.org/licenses/by-nc/4.0/).

$$\boldsymbol{m}(t) = P(t) \cdot \boldsymbol{B}_T(\boldsymbol{r}_T) \tag{4}$$

where $P(t)$ is a magnetic polarizability tensor (MPT) and $\boldsymbol{B}_T$ is the primary field at the target location $\boldsymbol{r}$ generated by the

transmitting coil at the location $\boldsymbol{T}$, and $\boldsymbol{r}_T = \boldsymbol{r}_R$ as transmitting and receiving coils are placed concentrically as shown in Fig. I. The MPT $P(t)$ is related to the orientation of the target, which is written as

$$P(t) = \boldsymbol{E} \begin{bmatrix} L_1(t) & & \\ & L_2(t) & \\ & & L_3(t) \end{bmatrix} \boldsymbol{E}^T \tag{5}$$

where $L_i(t)(i = 1,2,3)$ is the equivalent ith principal magnetic polarization strength of the target, and that the orientation matrix $\boldsymbol{E} = [\boldsymbol{e}_1\ \boldsymbol{e}_2\ \boldsymbol{e}_3]$, $\boldsymbol{e}_i(i = 1,2,3)$ is the orthonormal direction vector representing the ith principal direction of equivalent magnetic dipolar polarization with respect to a local coordinate system.

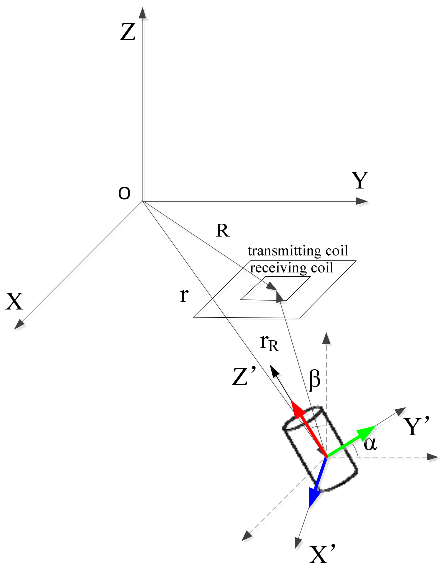

FIGURE I. SUBSURFACE TARGET COORDINATE SYSTEM

The magnetic field generated at $\boldsymbol{R}$ by the receiving coil with the unit current at $\boldsymbol{r}$ is

$$\boldsymbol{B}_R(\boldsymbol{r}_R) = \frac{\mu_0}{4\pi} \int_l \frac{\boldsymbol{dl} \times -\boldsymbol{r}_R}{|\boldsymbol{r}_R|^3} \tag{6}$$

Substituting (4) (5) into (3) and using (6), we have the final form of induced voltage measured at the receiving coil written as

$$V(\boldsymbol{r}_R, t) = \boldsymbol{B}_R{}^T(\boldsymbol{r}_R)\, \boldsymbol{E}l(t)\boldsymbol{E}^T \boldsymbol{B}_T(\boldsymbol{r}_T) \tag{7}$$

where superscript T denotes a transpose and we define the intrinsic responses of target $\boldsymbol{l}(t)$ as

$$\boldsymbol{l}(t) = \begin{bmatrix} \frac{dL_1(t)}{dt} & & \\ & \frac{dL_2(t)}{dt} & \\ & & \frac{dL_3(t)}{dt} \end{bmatrix} \tag{8}$$

and $\boldsymbol{l}(t)$ in (8) is related to only the characteristics of the target itself, such as shape, size, and material properties.

B. Classification Method

We propose the DE-LM joint inversion technique, which adopts the global parallel search algorithm DE to avoid convergence of any initial value to the local solution before using the LM to obtain the optimal solution. Next, we synthesize the parameters of the equivalent magnetic dipole intrinsic responses for subsurface targets classification, and the formulae are as follows.

$$\boldsymbol{Size} = \sum_{i=1}^{3} \boldsymbol{L_i(t_1)} \tag{9}$$

$$\boldsymbol{Decay} = \frac{\boldsymbol{L_i(t_n)}}{\max\limits_{i=1,2,3} |\boldsymbol{L_i(t_1)}|} \tag{10}$$

$$\boldsymbol{Symmetry} = \boldsymbol{min} \frac{\boldsymbol{1}}{\boldsymbol{n}} * \sum_{j=1}^{n} \frac{|\boldsymbol{L_p(t_j)} - \boldsymbol{L_q(t_j)}|^2}{|\boldsymbol{min}\{\boldsymbol{L_p(t_j)}, \boldsymbol{L_q(t_j)}\}|^2} \quad \boldsymbol{s.t}\ \{\boldsymbol{p}, \boldsymbol{q}\} \in \{\boldsymbol{1}, \boldsymbol{2}, \boldsymbol{3}\} \tag{11}$$

$$\boldsymbol{Ratio} = \begin{cases} \boldsymbol{min} \frac{\boldsymbol{1}}{\boldsymbol{n}} * \sum_{j=1}^{n} \frac{2\boldsymbol{L_m(t_j)}}{\boldsymbol{L_p(t_j)} + \boldsymbol{L_q(t_j)}}, & \boldsymbol{Decay} < \boldsymbol{threshold} \\ \boldsymbol{min} \frac{\boldsymbol{1}}{\boldsymbol{n}} * \sum_{j=1}^{n} \frac{\boldsymbol{L_p(t_j)} + \boldsymbol{L_q(t_j)}}{2\boldsymbol{L_m(t_j)}}, & \boldsymbol{otherwise} \end{cases}$$
$$\boldsymbol{s.t}\ \ \boldsymbol{min} \sum_{j=1}^{n} \frac{|\boldsymbol{L_p(t_j)} - \boldsymbol{L_q(t_j)}|}{\boldsymbol{min}\{\boldsymbol{L_p(t_j)}, \boldsymbol{L_q(t_j)}\}}, \{\boldsymbol{p}, \boldsymbol{q}, \boldsymbol{m}\} \in \{\boldsymbol{1}, \boldsymbol{2}, \boldsymbol{3}\} \tag{12}$$

where t_1 and t_n represent the central moments of the first and late time window.

The targets parameter information extracted from the above equations can be used to judge the size, material, symmetry and ratio of the targets, and to classify the subsurface targets.

III. RESULTS

We use the synthetic data to demonstrate the effectiveness of the method proposed herein. The 13 different targets including targets of interest, clutters and metal fragments are buried in 5m × 5m area with a measured point spacing of 50cm. The target parameters are shown in Table I. The experimental results show that, with 15% Gaussian white noise, the joint DE-LM inversion technique has the minimum residual sum of squares as compared with two stand-alone techniques, and it can bring convergence to the optimal solution each time.

TABLE I. PARAMETERS OF THE SUBSURFACE TARGETS

TARGET NUMBER	TARGET SIZE(CM)	MATERIAL	SHAPE
1	20*10*10	STEEL	BARREL
2	28*8.28*8.28	STEEL	BARREL
3	27*7.96*7.96	STEEL	BARREL
4	20*5*5	STEEL	BARREL
5	20*2.5*2.5	STEEL	BARREL
6	20*20*10	STEEL	PLATE
7	20*20*5	STEEL	PLATE
8	20*20*2.5	STEEL	PLATE
9	5*2.5*0.64	STEEL	IRREGULAR
10	1.3*2.5*0.64	STEEL	IRREGULAR
11	20*20*10	ALUMINUM	PLATE
12	20*20*5	ALUMINUM	PLATE
13	20*20*2.5	ALUMINUM	PLATE

Taking the target 1 as an example, in theory, the intrinsic response of the magnetic dipole 1 is greater than those of the dipoles 2 and 3, and the intrinsic responses of the magnetic dipoles 2 and 3 are basically identical due to the symmetry of the target. The convergence of three inversion techniques is shown in Fig. Ⅱ. In the inversion results of the three techniques, the intrinsic responses of the dipoles of the DE-LM joint inversion technique are closest to the target theoretical response, both LM and DE result in the wrong results via inversion, as shown in Fig. Ⅲ.

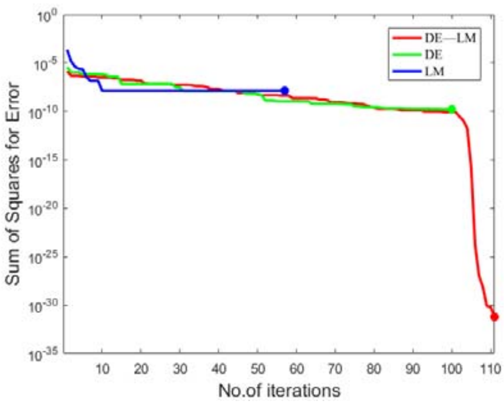

FIGURE II. THE CONVERGENCE OF THREE INVERSION TECHNIQUES.

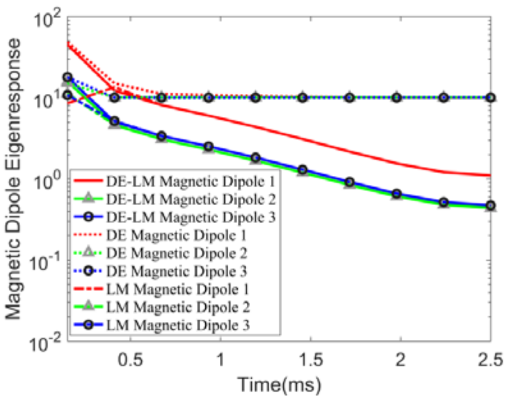

FIGURE III. THE INTRINSIC RESPONSES OF THREE INVERSION TECHNIQUES.

The corresponding parameters of the three inversion techniques are shown in Table II. The *Size* of the DE-LM inversion is 78.9876, which can be used to infer that the target volume is larger; the *Decay* is 0.0244, which can be adopted to infer that the material should be provided with smaller conductivity, such as steel. The *Symmetry* is 0.0089 and the *Ratio* is 2.5424, and it can be inferred that the target is axisymmetric and barrel-shaped. All of the four parameters agree well with the properties of the target 1, which proves the correctness of the targets classification method proposed herein. However, the classification results of LM and DE techniques all have errors, which prove the superiority of DE-LM joint inversion technique once more. The classification method of all targets adopts the DE-LM joint inversion technique.

TABLE II. SYNTHESIS PARAMETERS OF THREE INVERSION TECHNIQUES

INVERSION TECHNIQUE	SIZE	DECAY	SYMMETRY	RATIO
LM	70.5804	0.2129	0.0059	0.6220
DE	30.6802	0.0418	0.0044	0.6708
DE-LM	78.9876	0.0244	0.0089	2.5424

Fig. Ⅳ and Ⅴ show the parameter synthesis results of the 13 targets.

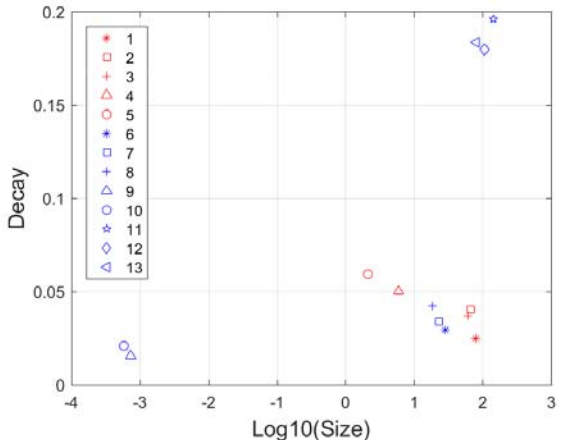

FIGURE Ⅳ. THE LOG10(SIZE)-DECAY FIGURE.

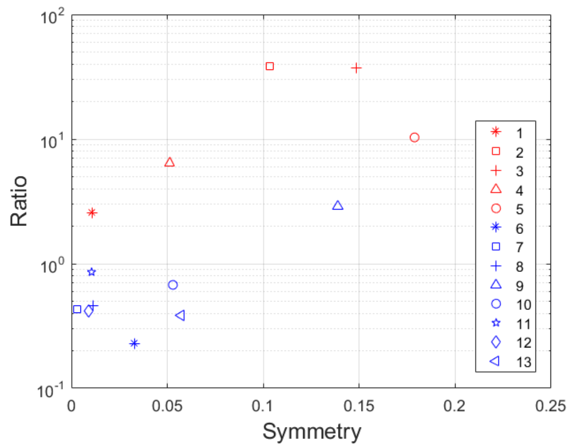

FIGURE Ⅴ. THE SYMMETRY-RATIO FIGURE.

1) It is found that the relative size of the target parameter $Size$ is consistent with the actual size of the targets;

2) The conductivity of aluminum is so large that the decay rate is slower than that of steel, and the extracted parameter $Decay$ is consistent with the nature of the targets and can be distinguished by Fig. IV with three large aluminum clutters (which have same volume as the steel barrel);

3) Target 9 and 10 are shallow metal fragments (small depths cause large responses, easily excavated as targets of interest), and it can be seen from the Fig. Ⅳ that their sizes are small so that they are judged as metal fragments rather than targets of interest;

4) Most targets are axisymmetric, and therefore, the extracted parameter $Symmetry$ is very small, consistent with the target property;

5) Taking the target materials into account before extracting the parameter $Ratio$, the results are consistent with the actual characteristics of the targets, and the clutters 6, 7 and 8 are excluded from the targets of interest.

Finally, we correctly identify all the 5 targets of interest from 13 buried targets with no any false targets occurred.

IV. CONCLUSION

A novel subsurface targets classification method based on DE-LM joint inversion technique is presented in this paper. The accuracy of the target shape estimation is greatly improved by the aid of the materials of the targets considered. The experimental results demonstrate that the method can bring convergence to the optimal solution each time and classify subsurface targets quickly and accurately.

ACKNOWLEDGMENT

This research work is supported by the Innovation Project of Chinese Academy of Sciences.

REFERENCES

[1] T. M. Grzegorczyk, J. P. Fernandez, F. Shubitidze, K. O'Neill, and B. E. Barrowes, "Subsurface electromagnetic induction imaging for unexploded ordnance detection," J. Appl. Geophys., vol. 79, pp. 38–45, Apr. 2012.

[2] Grimm, Robert E. "Time Domain Measurements and Modeling of UXO." Uxo Forum. 2001.

[3] L. R. Pasion and D. W. Oldenburg, "A discrimination algorithm for UXO using time domain electromagnetics," J. Eng. Environ. Geophys, vol. 6, no. 2, pp. 91–102, 2001.

[4] J. T. Smith and H. F. Morrison, "Estimating equivalent dipole polarizabilities for the inductive response of isolated conductive bodies," IEEE Trans. Geosci. Remote Sens., vol. 42, no. 6, pp. 1208–1214, Jun. 2004.

[5] L. P. Song, D. W. Oldenburg, L. R. Pasion, and S. D. Billings, "Transient electromagnetic inversion of multiple targets," Proc. SPIE, vol. 7303, pp. 73030R–73030R12, 2009.